AIP | Applied Physics Letters

Air-stable short-wave infrared PbS colloidal quantum dot photoconductors passivated with Al2O3 atomic layer deposition

Chen Hu, Alban Gassenq, Yolanda Justo, Kilian Devloo-Casier, Hongtao Chen, Christophe Detavernier, Zeger Hens, and Günther Roelkens

Citation: Applied Physics Letters **105**, 171110 (2014); doi: 10.1063/1.4900930
View online: http://dx.doi.org/10.1063/1.4900930
View Table of Contents: http://scitation.aip.org/content/aip/journal/apl/105/17?ver=pdfcov
Published by the AIP Publishing

Air-stable short-wave infrared PbS colloidal quantum dot photoconductors passivated with Al_2O_3 atomic layer deposition

Chen Hu,[1,2,3] Alban Gassenq,[1,2] Yolanda Justo,[2,3] Kilian Devloo-Casier,[4] Hongtao Chen,[1,2] Christophe Detavernier,[4] Zeger Hens,[2,3] and Günther Roelkens[1,2,a)]
[1]*Photonics Research Group-INTEC, Ghent University-imec, Sint-Pietersnieuwstraat 41, 9000 Ghent, Belgium*
[2]*Center for Nano-and Biophotonics, Ghent University, Sint-Pietersnieuwstraat 41, 9000 Ghent, Belgium*
[3]*Physics and Chemistry of Nanostructures Group, Ghent University, Krijgslaan 281-S3, B-9000 Ghent, Belgium*
[4]*Department of Solid State Sciences, Universiteit Gent, Krijgslaan 281-S1, 9000 Ghent, Belgium*

(Received 1 September 2014; accepted 21 October 2014; published online 30 October 2014)

A PbS colloidal quantum dot photoconductor with Al_2O_3 atomic layer deposition (ALD) passivation for air-stable operation is presented. Two different types of inorganic ligands for the quantum dots, S^{2-} and OH^-, are investigated. PbS/S^{2-} photoconductors with a cut-off wavelength up to 2.4 μm are obtained, and a responsivity up to 50 A/W at 1550 nm is reported. The corresponding specific detectivity is $\sim 3.4 \times 10^8$ Jones at 230 K. The 3-dB bandwidth of the PbS/S^{2-} and PbS/OH^- photodetectors is 40 Hz and 11 Hz, respectively. © *2014 AIP Publishing LLC*.
[http://dx.doi.org/10.1063/1.4900930]

The short-wave infrared (SWIR) wavelength region (1–2.5 μm) is important for spectroscopy and imaging applications. Detectors and cameras for this wavelength range are mainly based on epitaxial III-V materials.[1] The high material and integration cost of such devices prohibits large scale deployment, especially when used in a linear or two-dimensional focal plane array. Colloidal quantum dots (QDs) are a relatively new optoelectronic material that offers an alternative way to achieve SWIR photodetectors. This material—realized by hot injection synthesis and available in solution—can be integrated on any substrate, including silicon, using techniques such as spin casting,[2] inkjet printing,[3] and Langmuir-Blodgett (LB) deposition,[4] thus offering a route to the cost reduction of SWIR components. In addition, due to the quantum size effect, the QDs electrical and optical properties (absorption cut-off wavelength, luminescence wavelength) can be easily tuned by varying the QD size.[5] The interest in these materials is therefore not limited to photodetection[6] but also encompasses light emitting diodes [7] and photovoltaics.[8] Critical for photodetector and photovoltaic applications is the replacement of the long isolating organic ligands capping as-synthesized QDs by shorter moieties to enhance carrier mobility in QD films.[9] Also, making the colloidal QD devices air-stable is of key importance for a practical application.

In this study, we use atomic layer deposition (ALD) to deposit Al_2O_3 films on PbS colloidal QD films for passivation and implement air-stable SWIR photodetectors. Homogenous and crack-free QD films are obtained by a layer-by-layer (LBL) approach, where each cycle involves a QD layer deposition through dip coating, followed by a replacement of the native organic ligand by a metal-free inorganic ligand, such as OH^- and S^{2-} Ref. 10. Afterwards, a thorough cleaning procedure is used to remove impurities. One significant advantage of this approach is that there is no need for a stable QD dispersion with short ligands, and that the cracks formed during ligand exchange in the layer-by-layer approach are refilled in the next deposition step. For surface illuminated detectors, the QD films are formed on prefabricated interdigitated electrodes, where selective wet etching is used to pattern the QD film.[10] The resulting photodetectors are then passivated with an aluminum oxide coating through ALD.[11–14] Long term air-stable PbS colloidal QD photodetectors with a 2.4 μm cut-off wavelength are obtained this way.

Oleylamine (OlAm) terminated PbS QDs were synthesized based on the method developed by Cademartiri *et al.* and described in detail in Ref. 5. A stock solution was prepared by heating a mixture of 0.16 g (5 mmol) S in 15 ml of OlAm (technical, C18-content 80%–90%) under nitrogen for 30 min at 120 °C. In the first step of the synthesis, a mixture of 0.834 g (3 mmol) of $PbCl_2$ and 7.5 ml of OlAm in a three-neck flask was degassed under nitrogen for 30 min at 125 °C. Afterwards the mixed $PbCl_2$ solution was heated up to reach the required injection temperature, and then a mixture of 2.25 ml of OlAm-S stock solution (0.75 mmol of S) and 170 μl (375 μmol, half amount of S) of tri-n-octylphosphine (TOP) were injected into the flask. After injection the temperature dropped by 5–10 °C, and then the resultant growth temperature (160 °C) was maintained through the whole reaction. After growth for 2 h 30 min, the reaction was quenched by adding a mixture of 10 ml of toluene and 15 ml of MeOH. The QDs were separated from the reaction mixture by centrifugation and the obtained QD pellet was redispersed in 10 ml of toluene. After the synthesis, the OlAm ligands were replaced by oleic acid (OlAc) to obtain a ligand shell that withstands successive purification cycles.[10,15] The ligand exchange was realized by adding OlAc to a PbS QD in toluene suspension with a volume ratio of 1.5:10 (OlAc: toluene). Afterwards, the suspension was purified using methanol (MeOH) and toluene as the non-solvent and the solvent, respectively. Typically, the ligand exchange is repeated twice. The concentration of the resulting QD suspension was determined from the QD absorbance spectrum

a)Electronic mail: gunther.roelkens@intec.UGent.be

through the molar extinction coefficient at 400 nm ($17.06\,cm^{-1}/\mu M$).[5]

The fabrication of the PbS photodetectors started with the deposition of a 500 nm thick insulating SiO_2 layer with plasma enhanced chemical vapor deposition (PECVD) on a silicon substrate. Afterwards, a pair of interdigitated TiAu (10 nm Ti, 100 nm Au) finger electrodes was defined through optical lithography and lift-off. The electrodes were designed to be 2 μm wide and spaced 2 μm apart (limited by the resolution of the lithography system). Afterwards, QD films were deposited by LBL deposition, dipping the substrates with the prefabricated metal electrodes into a PbS QD dispersion in toluene with a QD concentration of 1 μM and pulling it out at a speed of 80 mm min^{-1}. After complete drying, the QD film was re-immersed into a solution of either $Na_2S{\cdot}9H_2O$ ($10\,mg\,ml^{-1}$) or KOH ($0.01\,mg\,ml^{-1}$) in formamide to exchange the OlAc ligands by S^{2-} or OH^- moieties respectively for the desired ligand exchange time, typically 60 s for S^{2-} and 10 s for OH^-. After that the sample was washed by immersing it twice in formamide and acetone, followed by a final dip in isopropanol to remove residual impurities introduced during ligand exchange. The resulting films were dried under nitrogen. A multi-layer film can be formed by repeating this dip coating/ligand exchange procedure. The photodetectors were fabricated by 15 times LBL deposition. Afterwards a selective wet-etching approach was used to realize micropatterned QD films on prefabricated electrodes,[10] resulting in PbS QD films of 130 μm by 104 μm. Then atomic layer deposition of Al_2O_3 was used to passivate the devices. Al_2O_3 was used since it is a very well characterized material in ALD and it is transparent in the SWIR. The depositions were carried out in a home-built hot wall ALD reactor. The ALD chamber was pumped by a turbomolecular pump to a base pressure of 10^{-4} Pa. Samples were introduced via a load lock and placed on a resistive heating element located at the center of the chamber. A thermal ALD process at 100 °C was used to grow Al_2O_3. The samples were sequentially exposed to 3 s of TMA (trimethylaluminum) and 3 s of water vapor at a pressure of $5{\cdot}10^{-1}$ Pa. 300 ALD cycles were performed, resulting in a 30 nm thick pinhole free alumina film (measured on a silicon reference by ellipsometry).[11]

A top view of a processed PbS QD photoconductor for surface illumination is shown in Figure 1(a). In this study, we used PbS QDs with an exciton peak wavelength at 2.09 μm. According to the PbS sizing curve this corresponds to an inorganic core diameter of 9 nm as confirmed by TEM measurements (Figure 1(b), inset).[15] Due to the size dispersion the QDs the absorption edge extends to about 2.4 μm (see Figure 1(b)). In order to investigate the relationship between the film thickness and the number of LBL deposition cycles, samples with 2, 4, 6, 8, and 10 LBL deposition cycles were realized. To determine the QD film thickness, we measured the average height profile of micropatterned QD films by atomic force microscopy (AFM), both before and after Al_2O_3 deposition (see Figures 1(c) and 1(d)). For both PbS/S^{2-} and PbS/OH^-, a linear trend can be observed amounting to a 6.5 nm and 5.5 nm thickness increase per LBL cycle, respectively. This is less than the diameter of a single nanocrystal, which is most likely related to the ligand exchange inducing a volume loss and particle clustering by removal of the long organic ligands. The resulting voids are then refilled in the following deposition cycle, which reduces the thickness increase per cycle. As shown in Figure 1(d), Al_2O_3 growth by ALD does not affect this thickness increase per deposition cycle (Figure 1(d)). This is due to the conformal nature of ALD, the ALD coating has been added over the complete device surface, retaining the underlying geometry.

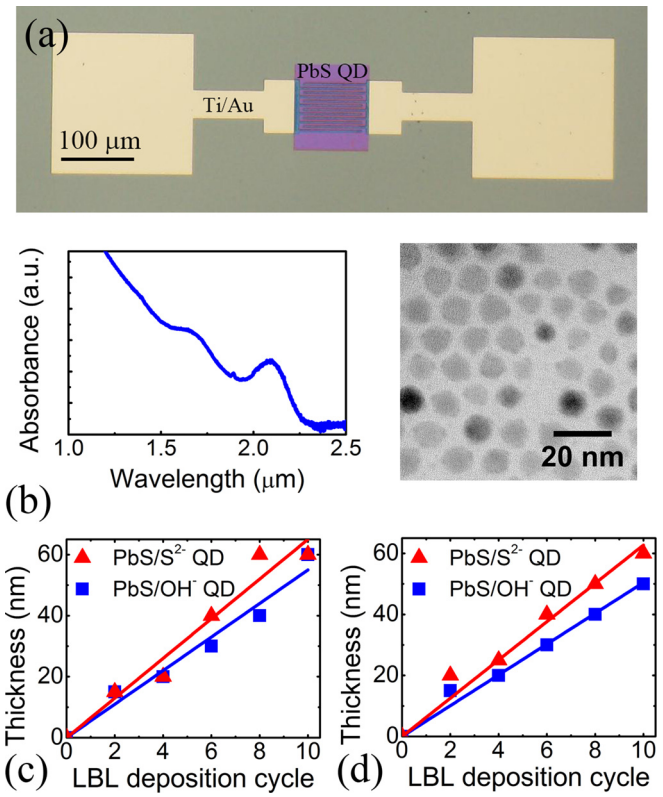

FIG. 1. (a) Top view of the PbS QD photoconductor. (b) Absorbance spectrum of OlAc-terminated colloidal PbS QDs used (solvent: tetrachloroethylene) and the corresponding TEM image. (c) Thickness of micropatterned PbS films as a function of the number of LBL cycles without Al_2O_3 deposition (d) The same, after Al_2O_3 deposition.

The current-voltage characteristics of PbS photoconductors under different illumination intensity were measured by surface illumination with a fiber coupled laser at 1550 nm. The I-V characteristics as a function of incident optical power for a PbS/S^{2-} and PbS/OH^- photoconductor with 15 LBL deposition cycles are shown in Figure 2. Under illumination, the S^{2-} terminated device resistance decreased from 3.30 kΩ in the dark to 1.09 kΩ under 11 W/cm^2 optical illumination intensity. After passivation with a 30 nm thick Al_2O_3 film, the dark resistivity became 28.0 kΩ and decreased to 4.18 kΩ under the same illumination intensity of 11 W/cm^2. As shown in Figures 2(c) and 2(d), similar results are obtained using OH^- terminated PbS QD detectors. The I-V characteristic difference between PbS/S^{2-} and PbS/OH^- photoconductors mainly comes from the different passivation ligands, which change the electronic coupling between the QDs. As TEM images illustrate in Ref. 10, after ligand exchange, the S^{2-} terminated QDs tend to connect epitaxially, opposed to the OH^- terminated QDs. The closer spacing of S^{2-} terminated QDs result in a higher electrical conductivity in these devices.

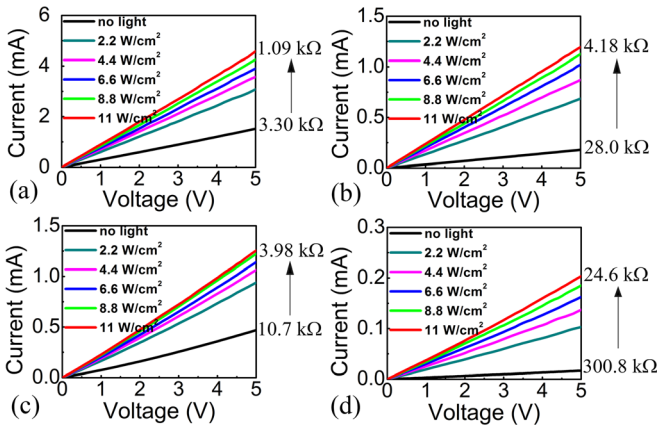

FIG. 2. Current–Voltage characteristics of processed PbS colloidal QD photoconductors: PbS/S^{2-} detector (a) without and (b) with 30 nm Al_2O_3 passivation; PbS/OH^- detector (c) without and (d) with 30 nm Al_2O_3 passivation.

The characteristics of the photodetectors based on unpassivated QD films were found to degrade with time, which we attribute to oxidation of the PbS QD surface. Overcoating the PbS QD films by Al_2O_3 proved to be an efficient way to avoid this degradation. Figures 3(a) and 3(b) show the dark current and photocurrent of the PbS/S^{2-} QD photodetector under 2.2 W/cm^2 illumination at 5 V bias as a function of time. The unpassivated device showed a pronounced progressive decay of both the dark current and the photocurrent. On the other hand, the response of the PbS/S^{2-} QD based photodetector passivated by a 30 nm Al_2O_3 film proved to be air-stable for 60 days at least. Moreover, although the ALD passivation led to a decrease in both dark current and photocurrent, which is currently not well understood, its responsivity exceeds that of the unpassivated device after 20 days in air. We thus conclude that the ALD deposition of Al_2O_3 can be used to passivated PbS QD films and form air-stable QD photodetectors.

The spectral response of the PbS photoconductors is shown in Figure 4(a) as measured with a fiber coupled tunable laser, under 5 V bias (1.1 W/cm^2 optical illumination intensity). A photoresponse extending to 2.4 μm was found for both PbS/S^{2-} and PbS/OH^- based detectors. Figure 4(b) shows the responsivity of the PbS/S^{2-} and PbS/OH^- QD photodetectors as a function of power level, clearly illustrating a nonlinear response of the device. The responsivity of the PbS/S^{2-} photodetector can reach more than 50 A/W for 100 nW optical power at 5 V bias. This photoconductive gain reflects a long carrier lifetime—probably resulting from trap states inside the QD film—compared to the carrier transit time

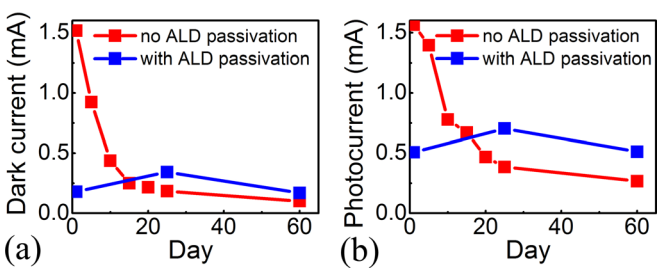

FIG. 3. PbS/S^{2-} QD photodetector dark current (a) and photocurrent under 2.2 W/cm^2 optical illumination (b) and 5 V bias as a function of time.

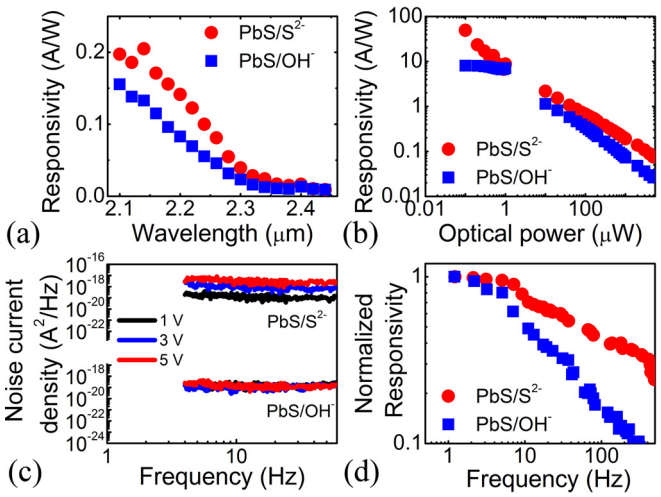

FIG. 4. (a) Spectral response as a function of wavelength; (b) responsivity as a function of optical illumination at 1550 nm (bias voltage 5 V) for the PbS/S^{2-} and PbS/OH^- QD photodetectors; (c) noise current density at different bias voltages for the PbS/S^{2-} and PbS/OH^- QD photodetectors at 230 K; (d) electrical frequency response (5 V bias).

between the electrodes. The power dependent responsivity is attributed to the filling of these long-lived trap states with increasing illumination power, which reduces the internal photoconductive gain.[3,16] For PbS/OH^- QD photodetector, a responsivity of 8 A/W is obtained under same conditions. The noise current density at 230 K of the ALD passivated PbS/S^{2-} and PbS/OH^- photoconductors measured at different bias is shown in Figure 4(c). A specific detectivity of 3.4×10^8 Jones and 2.3×10^8 Jones at 1550 nm is obtained under 5 V bias for PbS/S^{2-} and PbS/OH^- based detectors, respectively. The specific detectivity is found to be quasi independent of the bias voltage between 1 and 5 V. The frequency response of PbS/S^{2-} and PbS/OH^- photodetectors under 5 V bias is shown in Figure 4(d). The 3-dB bandwidth of the PbS/S^{2-} and PbS/OH^- detectors are 40 Hz and 11 Hz, respectively, which is compatible with basic imaging applications. The larger bandwidth of the PbS/S^{2-} devices is attributed to shorter carrier trap times in the quantum dot film.

PbS colloidal quantum dots were used to realize SWIR photoconductors. Air-stable devices with Al_2O_3 atomic layer deposition passivation were demonstrated. The QD films were prepared by a layer-by-layer approach to form a uniform colloidal QD film and two kinds of inorganic ligands, S^{2-} and OH^-, were investigated to facilitate carrier transport. PbS photodetectors with a cutoff wavelength of 2.4 μm are obtained. For PbS/S^{2-} photodetectors, a responsivity up to 50 A/W and a specific detectivity of 3.4×10^8 Jones are obtained at 1550 nm and 230 K. For PbS/OH^- photodetectors, the responsivity is ~8 A/W and the corresponding specific detectivity is $\sim 2.3 \times 10^8$ Jones under the same measurement conditions. The 3-dB bandwidth of the PbS/S^{2-} and PbS/OH^- photodetector is 40 Hz and 11 Hz respectively, obtained under 1.1 W/cm^2 illumination at 2250 nm. This approach can become a viable approach to realize low-cost imaging sensors and single pixel photodetectors.

This work was supported by the FWO (NanoMIR project), EU-FP7 (ERC-MIRACLE), BelSPo (IAP 7.35 photonics@be) and Ghent University (BOF-GOA

01G01513). We acknowledge the assistance from Steven Verstuyft during the device fabrication.

[1]B. Chen, W. Y. Jiang, J. Yuan, A. L. Holmes, and B. M. Onat, IEEE Photonics Technol. Lett. **23**(4), 218–220 (2011).
[2]S. Coe-Sullivan, J. S. Steckel, W.-K. Woo, M. G. Bawendi, and V. Bulović, Adv. Funct. Mater. **15**, 1117–1124 (2005).
[3]M. Böberl, M. V. Kovalenko, S. Gamerith, E. J. W. List, and W. Heiss, Adv. Mater. **19**, 3574–3578 (2007).
[4]Y. Justo, I. Moreels, K. Lambert, and Z. Hens, Nanotechnology **21**, 295606 (2010).
[5]I. Moreels, K. Lambert, D. Smeets, D. D. Muynck, T. Nollet, J. C. Martin, F. Vanhaecke, A. Vantomme, C. Delerue, G. Allan, and Z. Hens, ACS Nano **3**, 3023–3030 (2009).
[6]T. Rauch, M. Böberl, S. F. Tedde, J. Fürst, M. V. Kovalenko, G. Hesser, U. Lemmer, W. Heiss, and O. Hayden, Nat. Photonics **3**, 332–336 (2009).
[7]B. N. Pal, Y. Ghosh, S. Brovelli, R. Laocharoensuk, V. I. Klimov, J. A. Hollingsworth, and H. Htoon, Nano lett. **12**, 331–336 (2012).
[8]H. Liu, D. Zhitomirsky, S. Hoogland, J. Tang, I. J. Kramer, Z. Ning, and E. H. Sargent, Appl. Phys. Lett. **101**, 151112 (2012).
[9]E. Talgorn, M. A. de Vries, L. D. A. Siebbeles, and A. J. Houtepen, ACS Nano **5**, 3552–3558 (2011).
[10]C. Hu, T. Aubert, Y. Justo, S. Flamee, M. Cirillo, A. Gassenq, O. Drobchak, F. Beunis, G. Roelkens, and Z. Hens, Nanotechnology **25**, 175302 (2014).
[11]K. Lambert, J. Dendooven, C. Detavernier, and Z. Hens, Chem. Mater. **23**(2), 126–128 (2011).
[12]S. H. Kim, P. H. Sher, Y. B. Hahn, and J. M. Smith, Nanotechnology **19**, 365202 (2008).
[13]A. Pourret, P. Guyot-Sionnest, and J. W. Elam, Adv. Mater. **21**, 232–235 (2009).
[14]R. Ihly, J. Tolentino, Y. Liu, M. Gibbs, and Matt Law, ACS Nano **5**, 8175–8186 (2011).
[15]I. Moreels, Y. Justo, B. D. Geyter, K. Haustraete, J. C. Martins, and Z. Hens, ACS Nano **5**, 2004–2012 (2011).
[16]G. Konstantatos and E. H. Sargent, Nat. Nanotechnol. **5**, 391–400 (2010).